ISO OBSERVATIONS OF SPIRALS: MODELLING THE FIR EMISSION

S. Bianchi, P.B. Alton, J.I. Davies

Department of Physics & Astronomy, Cardiff University,
PO Box 913, Cardiff CF2 3YB, U.K.

ABSTRACT

ISO observations at 200μm have modified our view of the dust component in spiral galaxies. For a sample of seven resolved spirals we have retrieved a mean temperature of 20K, about 10K lower than previous estimates based on IRAS data at shorter wavelengths. Because of the steep dependence of far-infrared emission on the dust temperature, the dust masses inferred from ISO fluxes are a factor of 10 higher than those derived from IRAS data only, leading to gas-to-dust ratios close to the value observed in the Galaxy. The scale-length of the 200μm emission is larger than for the IRAS 100μm emission, with colder dust at larger distances from the galactic centre, as expected if the interstellar radiation field is the main source of dust heating. The 200μm scale-length is also larger than the optical, for all the galaxies in the sample. This suggests that the dust distribution is more extended than that of the stars.

A model of the dust heating is needed to derive the parameters of the dust distribution from the Far-Infrared (FIR) emission. Therefore, we have adapted an existing radiative transfer code to deal with dust emission. Simulated maps of the temperature distribution within the dust disk and of the dust emission at any wavelength can be produced. The stellar spectral energy distribution is derived from observations in the ultraviolet, optical and near infrared. The parameters of the dust distribution (scale-lengths and optical depth) are chosen to reproduce the observed characteristics of the FIR emission, i.e. the shape of the spectrum, the flux and the spatial distribution. We describe the application of the model to one of the galaxies in the sample, NGC 6946.

Key words: ISOPHOT; spiral galaxies; extended emission; cold dust; FIR: observations; FIR: models.

1. INTRODUCTION

Diffuse dust is responsible for the internal extinction in a spiral galaxy. The grains of this diffuse component are heated up to temperatures $T < 20\,\mathrm{K}$ by the mean galactic Interstellar Radiation Field (ISRF; Reach et al. 1995). Emission from cold dust peaks at $\lambda > 150\mu$m, while dust in circumstellar regions is hotter and emits preferentially at shorter wavelengths. The link between extinction and cold dust is revealed by the similar values of the gas-to-dust mass ratio retrieved in the Galaxy from independent studies of extinction and emission. Using mean dust properties (Hildebrand 1983;Whittet1992), a value of 130 can be derived from the correlation between the hydrogen column density and the B-V colour excess (Bohlin et al. 1978). From the Galactic FIR emission at $\lambda > 100\,\mu$m observed by the instrument DIRBE aboard the satellite COBE, Sodroski et al. (1994) derived a mean value of 160.

Until recently, the main source of FIR data for spiral galaxies has come from the IRAS satellite. Because of its limited spectral coverage ($\lambda < 120\mu$m), IRAS was not able to detect cold dust. Devereux & Young (1990) measured the gas-to-dust ratio for a sample of 58 spiral galaxies, using the IRAS 60 μm and 100 μm fluxes. A mean value of 1080 was derived, almost an order of magnitude larger than in the Galaxy. Assuming that the Galaxy is an average spiral, they explained the discrepancy with 90 per cent of the dust mass being at $T \sim 15\,\mathrm{K}$, too cold to be detected by IRAS.

Therefore, observations at longer wavelengths are essential to detect cold dust and to trace the internal extinction in a spiral galaxy. In this paper we describe ISOPHOT (Lemke et al. 1996) observations at 200 μm of a sample of seven spiral galaxies. An extended cold dust emission has been revealed (Section 2.). A model of FIR emission has been built to derive the parameters of the dust distribution from the observed properties of dust emission (Section 3.). A summary and a discussion of the results are given in Section 4.

2. ISO OBSERVATIONS OF SPIRALS

We give in this section a summary of the ISOPHOT 200 μm observations and results. A full description is presented in Alton et al. (1998).

Eight objects were observed with ISOPHOT, seven spiral galaxies and one irregular. The targets were selected to be representative of quiescent objects with normal FIR-to-blue luminosity ratio ($L_{FIR}/L_B < 1$, Soifer et al. 1987) and to have large apparent sizes ($\sim$ 10 arcmin), to be resolved by the ISO beam

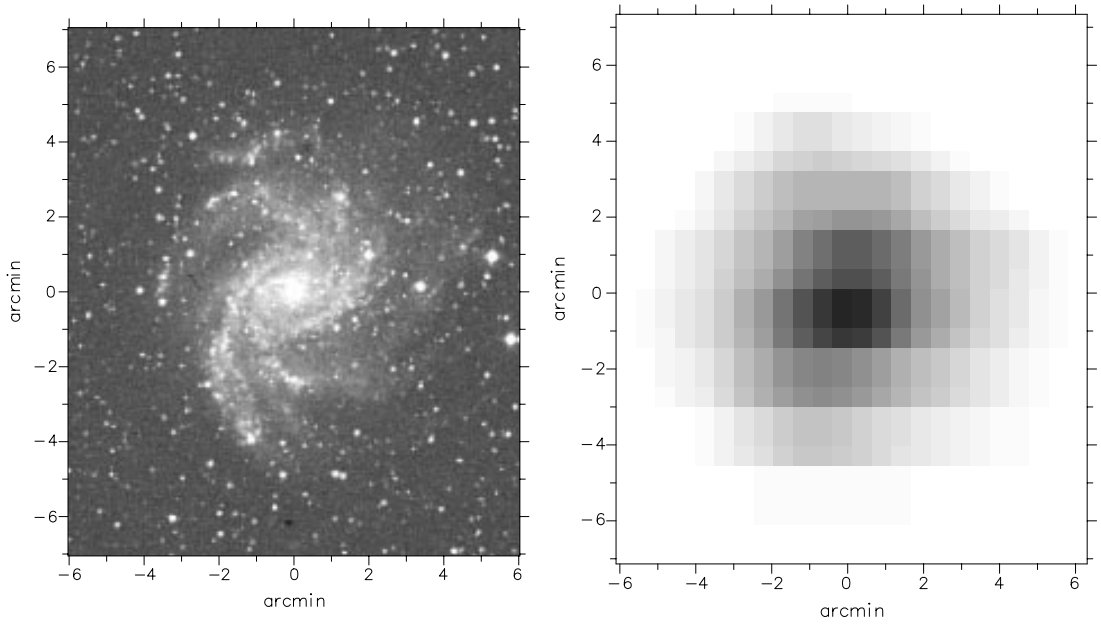

Figure 1. Images of the spiral galaxy NGC6946, in the B-band (left) and at 200 μm (right). Images are from Alton et al. (1998)

(FWHM=117 arcsec, Tuffs et al. 1996). B-band images were also obtained, together with resolution enhanced HiRes IRAS images at 60 and 100 μm (Rice1993). The ISOPHOT images are similar in morphology to the 100 μm HiRes, that have a comparable resolution. IRAS and B-band images were convolved to the ISO resolution and registered with the 200 μm images. As an example, we present in Figure 1 a full-resolution B-band image and a 200 μm image for one of the objects of the sample, the spiral galaxy NGC 6946.

Total integrated fluxes at 60, 100 and 200 μm were used to derive dust temperatures and masses. As for the dust emissivity, the form $Q_{em}(\lambda) = Q_{em}(\lambda_0) \times (\lambda/\lambda_0)^{-\beta}$ was chosen, allowing for two different wavelength dependences, β=1 and 2, and using $Q_{em}(\lambda_0)$ from Hildebrand (1983). After computing the dust mass, gas-to-dust mass ratios were derived using the total (atomic+molecular) gas masses listed by Devereux & Young (1990). Two set of calculation were carried out: the *IRAS view*, using only the 60 and 100 μm fluxes from IRAS; and the *ISO view*, using the 100 μm IRAS flux and the 200 μm ISO flux. The mean values of dust temperatures and gas-to-dust mass ratios over the observed sample are presented in Table 1.

Clearly, a larger amount of cold dust is revealed using the 200 μm data. Dust temperatures from the *ISO view* are colder by almost 10 degrees, and the gas-to-dust ratios are smaller by one order of magnitude, with respect to the *IRAS view*. The values for the gas-to-dust ratio are similar to the Galactic. The calibration of ISOPHOT is still uncertain. An integrated flux at 200 μm was derived for NGC 6946 from the observations of Engargiola (1991). The ISO flux for the same galaxy is larger by 30 per cent. The same result is obtained comparing the observed 200 μm background with that extrapolated from 100 μm, using a Galactic spectrum at high latitude from Reach et al. (1995). However, even accounting for an overestimation of the ISOPHOT calibration (results in brackets in Table 1), a larger quantity of cold dust is revealed by the *ISO view*.

Uncertainties on the calibration do not affect the results about the spatial distribution of FIR emission. Azimuthally averaged profiles were obtained for the optical and FIR smoothed images, and the exponential scale-lengths were measured between 1.5 arcmin and 3.5 arcmin. The mean scale-lengths for the seven spirals in the sample are presented in Table 2, normalised to the 200 μm value. The larger 200 μm scale-length with respect to the other FIR images shows that dust is colder at larger radii, consistently with dust grains heated by a diffuse ISRF of higher intensity in the centre of the galaxy. The 60 μm scale-length is similar to the 100 μm, a result also observed in the Galaxy (Sodroski et al. 1989) and explained with emission from small grains whose heating con-

Table 1. Mean temperatures and gas-to-dust ratios for the observed sample, derived for the IRAS view *and the* ISO view*, for two choices of the emissivity spectral index β. Values in brackets allow for an overestimation of the ISO fluxes by 30 per cent.*

	β	IRAS	ISO
$\langle$T(K)$\rangle$	1	34	21 (24)
	2	28	18 (19)
$\langle$Gas-to-Dust$\rangle$	1	2800	230 (494)
	2	5100	220 (446)

Table 2. Mean scale-lengths of the sample

60/200	0.57±0.05
100/200	0.56±0.04
B/200	0.79±0.05

ditions do not depend heavily on the ISRF gradient. The most striking results is the smaller B band scale-length with respect to that at 200 μm. If the dust distribution is similar to the stellar, the scale-length of FIR emission should be smaller than the optical, because the dust temperature is higher in the centre of the disk. Therefore, the larger 200 μm scale-length could be a hint for a dust distribution more extended than the stellar. Extended dust distributions also emerge from models of COBE emission at 140 μm and at 240 μm (Davies et al. 1997) and from fits of surface brightness in edge-on galaxies (Xilouris et al. 1999).

To check for the influence of transient effects along the scan direction, the galaxies were divided in four quadrants and the scale-lengths analysis repeated only on the two quadrants perpendicular to the scan direction. The same result was obtained.

3. MODELLING THE FIR EMISSION

In this section we briefly describe a model of FIR emission in spiral galaxies. The main purpose of the model is the derivation of the geometrical and optical parameters of the dust distributions through a comparison of simulations with observed FIR emission. In particular, we wanted to test the hypothesis that the extended dust emission described in Section 2. is due to an extended distribution of dust. A detailed description of the model and its results is deferred to a forthcoming paper (Bianchi, Davies & Alton 1999).

3.1. Description of the model

The model is based on a simplified version of the Monte Carlo radiative transfer code of Bianchi, Ferrara & Giovanardi (1996). The Monte Carlo method allows for a correct treatment of multiple scattering in geometries typical of spiral galaxies. For the models presented here, we use a double exponential disk geometry for both stars and dust, although the code is able to work with other distributions. The stellar and dust disk are geometrically defined by the radial and vertical scale-lengths. The opacity of the dust disk is defined by the face-on optical depth through the centre, τ_V. We used empirical dust properties for absorption and scattering (Gordon, Calzetti & Witt 1997)

The code is monochromatic. Simulated images for a particular wavelength are produced, together with a map of the energy absorbed by dust from starlight at that wavelength. Therefore, to obtain a map of the total energy absorbed by dust from the whole stellar Spectral Energy Distribution (SED), simulations are produced for 17 wavelengths bands covering the spectral range of stellar emission, from the ionization limit to the Near-Infrared.

The main aim of this work is the modelling of the FIR emission, that is produced by grains heated at thermal equilibrium. Since part of the absorbed energy is re-emitted in the Mid-Infrared by transiently heated small grains, a correction is applied to subtract their contribution from the absorbed energy map. The correction is derived from the absorption efficiency of small grains in the dust model of Désert, Boulanger & Puget (1990).

From the corrected absorbed energy map the temperature distribution along a meridian plane of the galaxy model is retrieved. A key quantity for this calculation is the emissivity. We have derived the emissivity value (Bianchi, Davies & Alton 1999) from maps of Galactic FIR emission, temperature and extinction (Schlegel, Finkbeiner & Davis 1998), assuming a spectral dependence as measured on high signal-to-noise FIR spectra of the Galactic plane (Reach et al. 1995).

Images of FIR emission are then produced from the temperature maps and dust distribution, integrating along specific line of sights. In this paper we describe an application to the spiral galaxy NGC 6946. Simulated optical and FIR images have been produced for the inclination of 34°, appropriate for the galaxy (Athanassoula, Garcia-Gomez & Bosma 1993), for several star-dust configurations. We have adopted a distance of 5.5 Mpc (Tully 1988) for the galaxy; an intrinsic *unextinguished* stellar radial scale-length $\alpha_\star = 2.5\,$kpc (derived from a K-band image); a radial/vertical scale-lengths ratio $\alpha_\star/\beta_\star = 14.4$ (a mean value derived from the compilation of vertical scale-lengths for different stellar types of Wainscoat et al. (1992)).

3.2. Results

We first tried a model with a *standard* distribution for the dust disk, i.e. with the dust radial scale-length of the same dimension as the stellar ($\alpha_d = \alpha_\star$) and vertical scale-length one half of the stellar ($\beta_d = 0.5\beta_\star$). The choice of the dust vertical scale-length is mainly dictated by the observation of extinction lanes in edge-on galaxies, that cannot be explained with dust distribution thicker than the stellar.

The SED of the stellar and dust emission are presented in Figure 2 for standard models of different τ_V. The optical data-points for the stellar emission are from Engargiola (1991) and represent the flux inside the B-band half-light aperture (5 arcmin diameter). UV fluxes inside the same aperture are derived from Rifatto, Longo & Capaccioli (1995). FIR fluxes inside the same aperture are derived from IRAS HiRes images and from the 200 μm ISO image. The 160 μm flux from Engargiola (1991) has been included as well. The simulated optical and UV images were integrated inside the B-band half light radius (also derived from the simulation) and the fluxes normalised to the observed values. The solid line in Figure 2 represent this SED of the observed stellar emission. The SED of the FIR emission (and that of the intrin-

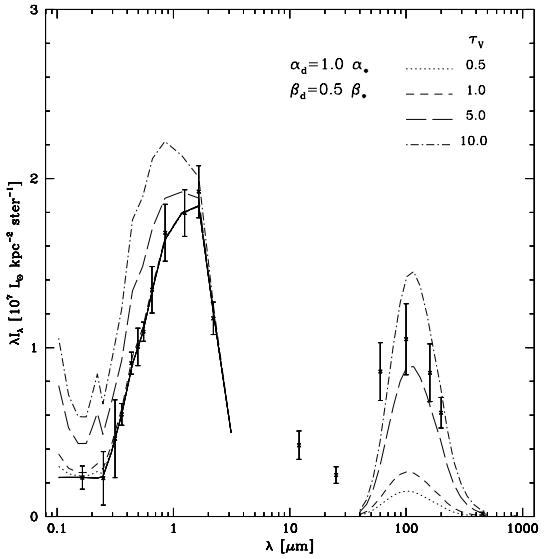

Figure 2. Optical and FIR SEDs for standard models ($\alpha_d = \alpha_\star$, $\beta_d = 0.5\beta_\star$) of different optical depths.

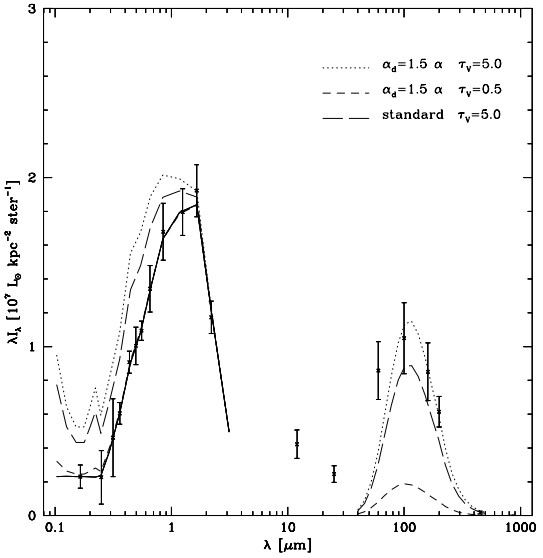

Figure 3. Optical and FIR SEDs for extended models ($\alpha_d = 1.5\alpha_\star$, $\beta_d = 0.5\beta_\star$) of optical depths $\tau_V = 0.5$ and $\tau_V = 5.0$. The standard model with $\tau_V = 5.0$ is also shown, for comparison.

sic, unextinguished, stellar radiation) are presented for models of different optical depths.

The SEDs of FIR radiation in Figure 2 show that only optically thick models ($\tau_V \sim 5$) can provide the observed amount of energy absorbed (and emitted) by dust. As for the scale-length of FIR emission, they increase with the optical depth. However, the B band scale-length increases with extinction as well. Because of this, the smaller value for the B/200 scale-lengths ratio occurs for optically thin model with $\tau_V = 0.5$ (1.4 vs 0.9 measured for NGC 6946). The temperature distributions are quite similar for any of the dust disk models. The temperature distribution on the meridian plane for the standard model with $\tau_V = 5.0$ is presented in the top panel of Figure 5. The model temperatures are compatible with those observed in the Galaxy (Sodroski et al. 1997) and on NGC 6946 itself (Davies et al. 1999).

Xilouris et al. (1999) modelled the surface brightness of a sample of seven edge-on galaxies with a double exponential geometry for dust and stars. The extinction lane is well fitted if the dust distribution is thinner and has a larger radial scale-length than the stellar ($\langle\alpha_d/\alpha_\star\rangle = 1.5, \langle\beta_d/\beta_\star\rangle = 0.5$). The dust disk are found to be optically thin, with a mean $\tau_V = 0.5$. Figure 4 shows the result for the case with extended disk. Despite the internal extinction has increased, still optically thick models are needed to absorb the right amount of energy. In an extended model, larger amounts of colder dust are present in the outer skirts of the disk (Figure 5) and this causes an increase in the FIR scale-lengths. However, the increase in the B-band scale-length due to extinction compensates for the larger FIR scale-lengths and the B/200 scale-lengths ratios are larger then observed. The smaller value (1.15) is again achieved for the optically thin case with $\tau_V = 0.5$. The models of COBE emission of Davies et al. (1997) suggest that the dust distribution is more extended then the stellar also in the vertical direction ($\beta_d = 2\beta_\star$). The inclusion of a thicker dust disk, however, does not modify the trend seen for the other models.

Since the molecular gas distribution of NGC 6946 follow closely the emission detected by IRAS, Davies et al. (1999) suggested that the broader 200 μm profile could be due to a more extended dust distribution associated with the atomic gas. Tacconi & Young (1986) report the column density of molecular and atomic hydrogen as a function of the galactocentric distance. The molecular gas has a steep profile, with an exponential scale-length $\approx 1\,\alpha_\star$. The atomic gas distribution has a dip in the centre, reaching a maximum at $\approx 2\,\alpha_\star$, then declining exponentially with a scale-length $\approx 3\,\alpha_\star$. The atomic and molecular phases have the same mass, but the former has a much broader distribution. A model with two dust disk mimicking the gas distributions is presented in Figure 4. As central face-on optical depth we choose τ_V^m=5 for the dust associated with the molecular gas, and τ_V^a=5 for the dust associated with the atomic phase. The adopted optical depths were derived using the correlation between extinction and gas column density (Bohlin et al. 1978) and a standard extinction law for the Galaxy (Whittet1992).

Despite the large extent of the disk associated with the atomic gas, the FIR emission in the model is dominated by the optically thick disk associated with the molecular phase. The behaviour of the double disk model is therefore similar to that of a standard model with τ_V=5. A good fit can be found only for the SED while the B/200 scale-length ratio is larger than observed. Interestingly, a better match of both FIR emission and scale-lengths ratio can be found for a single disk model, of the same scale-length of the one previously used for the atomic gas. An optical depth τ_V=3 is needed to match the observed

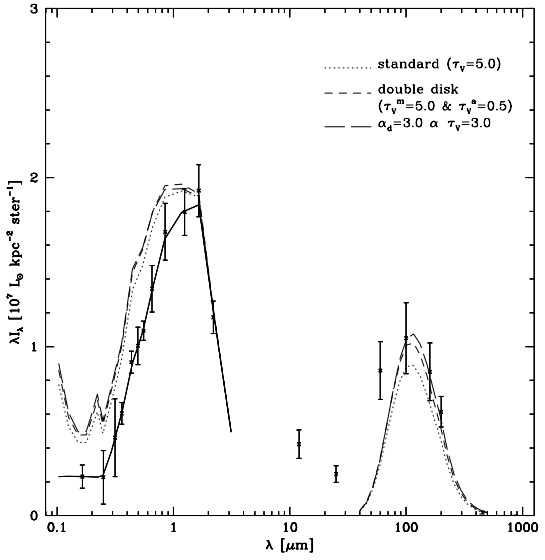

Figure 4. Optical and FIR SEDs for the double disk model, and for a single disk model with $\alpha_d = 3\alpha_\star$ and τ_V=5.0. The standard model with $\tau_V = 5.0$ is also shown, for comparison.

fluxes (Figure 4). The bottom panel of Figure 5 shows the temperature distribution for this model: increasing the dust scale-length with respect to the stellar results in larger amounts of colder dust in regions of low intensity ISRF. The FIR scale-length has increased enough to compete with the change in the B-band scale-length due to extinction and the resulting B/200 scale-length ratio is now slightly smaller than 1.

4. SUMMARY & CONCLUSIONS

ISO observations of a sample of seven spiral galaxies at 200 μm have revealed large amounts of cold dust (Alton et al. 1998). The FIR emission is found to have a larger scale-length than the optical ($\langle\alpha_B/\alpha_{200}\rangle \approx 0.8$), thus suggesting a broader distribution for dust than for stars.

We produced a model for the radiative transfer and FIR emission for geometries typical of a spiral galaxy. We applied the model to the observations of NGC 6946. For all the model explored, an optically thick dust distribution (with central face-on optical depth $\tau_V \sim 5$) is necessary to match the FIR spectrum. However, optically thick models fail to reproduce the observed ratio of B-band and 200 μm scale-lengths. For models with dust radial scale-length larger than the stellar by a factor 1.5, as suggested by fitting of surface brightness in edge-on galaxies, the optical-FIR scale-lengths ratio is closer to the observed value only in optically thin cases. A better fit of both FIR spectrum and spatial distribution of emission, in the optically thick case, can be reached only for $\alpha_d/\alpha_\star \geq 3$.

A few approximations have been adopted in this work. We have tested that the results are non qualitatively modified by: the neglect of the ionising stellar continuum; the presence of a small stellar bulge; the assumption of a single stellar vertical scale-length, instead of having a thinner stellar disk for young objects (Bianchi, Davies & Alton 1999) emitting preferentially at smaller λ. We have also assumed a single stellar radial scale-length at any λ, following the idea that colour gradients are mainly produced by dust extinction (Peletier et al. 1995). De Jong (1996) claims that extinction cannot explain the colour gradients observed in a sample of 86 spiral galaxy, for *reasonable* models of galactic disks. However, this definitions does not seem to include models with dust scale-lengths larger than the stellar, that have colour gradients as large as the observed.

A major assumption in the radiative transfer model is that of a smooth distribution, both for stars and dust. Clumping may be able to explain the paradox of needing both optically thick and optically thin distributions, to reproduce the FIR spectrum and scale-lengths ratio, respectively. Dust associated with the gas in molecular clouds may be responsible for most of the FIR emission, if large amounts of energy are absorbed from embedded stars. On the other hand, an optically thin distribution correlated to the atomic gas will be able to explain the observed spatial distribution of FIR emission. The galaxy may look as optically thin, when seen face-on, as derived from the surface brightness fits of Xilouris et al. (1999).

Such a scenario, however, does not seem to be supported by observations. For large objects with a well resolved clump structure, like the Milky Way and M31, only a 30 per cent of the FIR emission comes from star-forming regions embedded in molecular clouds (Sodroski et al. 1997; Xu & Helou 1996). It is then difficult to evaluate the effect of clumping on extinction and FIR emission. A study of the influence of clumping on the radiative transfer through a galactic disk is presented by Bianchi et al. (1999). It is found that clumping affects only marginally the radiative transfer. It would therefore be difficult for clumpy dust associated with molecular clouds to pass "undetected" in surface brightness fits. However, results depend highly on the description adopted for the clumps distribution. A description appropriate to the molecular distribution of NGC 6946, rather than the Galactic adopted in Bianchi et al. (1999), may produce different results. A proper model of FIR emission for a clumpy dust distribution is therefore needed to confirm the prediction of the last paragraph.

REFERENCES

Alton, P. B., Trewhella, M., Davies, J. I., et al. 1998, A&A, 335, 807

Athanassoula, E., Garcia-Gomez, C., Bosma, A. 1993, A&AS, 102, 229

Bianchi, S., Ferrara, A., Giovanardi, C. 1996, ApJ, 465, 127

Bianchi, S., Davies, J. I., Alton, P. B. 1999a, A&A, 344, L1

Bianchi, S., Davies, J. I., Alton, P. B. 1999b, in preparation

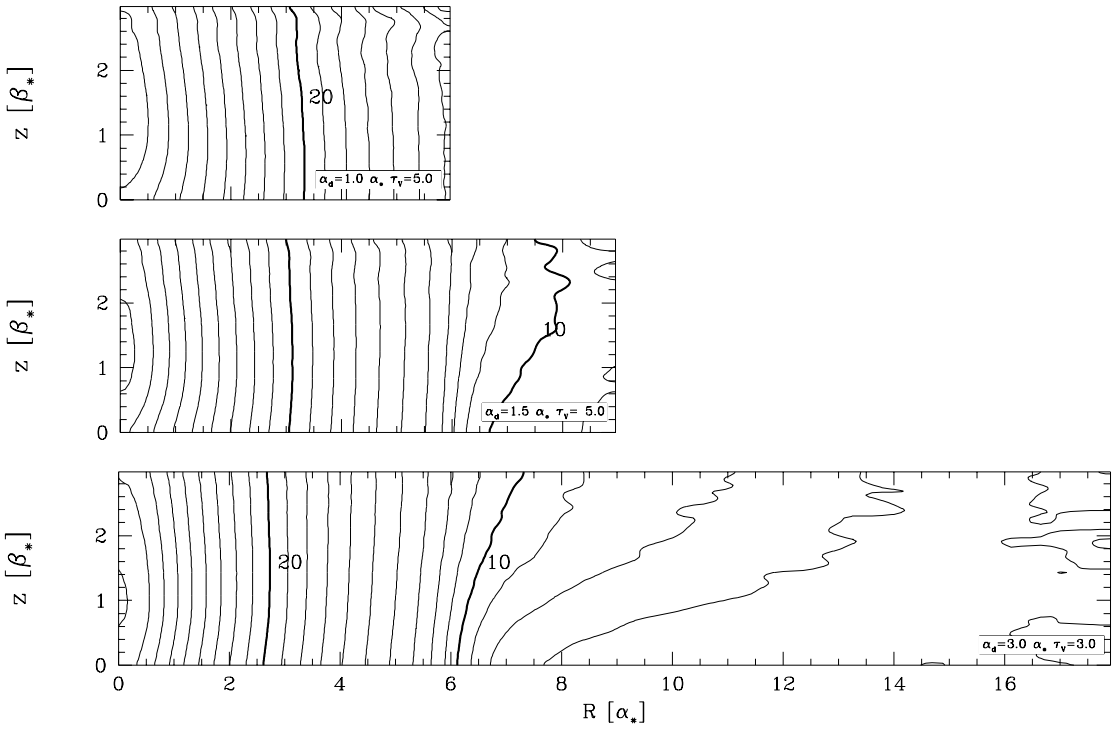

Figure 5. Temperature distribution on the meridian plane for the standard model with $\tau_V = 5$ (top panel) and the extended model with $\alpha_d = 1.5\alpha_\star$ and $\tau_V = 5$ (central panel). The bottom panel presents the temperature distribution for the extended model with $\alpha_d = 3.0\alpha_\star$ and $\tau_V = 3$. Contours are plotted every 1K and highlighted by a thicker line for the values of 10K and 20K. The scale on the x and y axes are different ($\alpha_\star = 14.4\beta_\star$). Dust and stellar disks are truncated at six scale-lengths.

Bianchi, S., Ferrara, A., Davies, J. I., Alton, P. B. 1999, MNRAS, accepted, astro-ph/9909395

Bohlin, R. C., Savage, B. D., Drake, J. F. 1978, ApJ, 224, 132

Davies, J. I., Trewhella, M., Jones, H., Lisk, C., Madden, A., Moss J. 1997, MNRAS, 288, 679

Davies, J. I., Alton, P. B., Trewhella, M., Evans, R., Bianchi, S. 1999, MNRAS, 304, 495

Désert, F. X., Boulanger, F., Puget, J. L. 1990, A&A, 237, 215

Devereux, N. A., Young, J. S. 1990, ApJ, 359, 42

De Jong R. 1996, A&A, 313, 377

Engargiola, G. 1991, ApJS, 76, 875

Gordon, K. D., Calzetti, D., Witt, A. N. 1997, ApJ, 487, 625

Hildebrand, R. H. 1983, QJRAS, 24, 267

Lemke, D., Klaas, U., Abolins, J., et al. 1996, A&A, 315, L64

Peletier, R., Valentijn, E., Moorwood, A., Freudling, W., Knapen, J., Beckman, J. 1995, A&A, 300, L1

Reach, W. T., Dwek, E., Fixsen, D. J. et al., 1995, ApJ, 451, 188

Rice, W. 1993, AJ, 105, 67

Rifatto, A., Longo, G., Capaccioli, M. 1995, A&AS, 109, 341

Schlegel, D. J., Finkbeiner, D. P., Davis, M. 1998, ApJ, 500, 525

Sodroski, T. J., Dwek, E., Hauser, M. G., Kerr, F. J. 1989, ApJ, 336, 762

Sodroski, T. J., Bennett, C., Boggess, N., et al. 1994, ApJ, 428, 638

Sodroski, T. J., Odegard, N., Arendt, R. G., et al. 1997, ApJ, 480, 173

Soifer, B. T., Sanders, D. B., Madore, B. F., et al. 1987, ApJ, 320, 238

Tacconi, L. J., Young, J. S. 1986, ApJ, 308, 600

Tully, R. B. 1988. Nearby galaxies catalog. Cambridge University Press, Cambridge

Tuffs, R. J., Lemke, D., Xu, C., et al. 1996, A&A 315, L149

Wainscoat, R. J., Cohen, M., Volk, K., Walker, H. J., Schwartz, D. E. 1992, ApJS, 83, 111

Whittet, D. C. B. 1992. Dust in the Galactic Environment. Institute of Physics Publishing, Bristol

Xilouris, E. M., Byun, Y. I., Kylafis, N. D., Paleologou, E. V., Papamastorakis, J. 1999, A&A, 344, 868

Xu, C., Helou, G. 1996, ApJ, 456, 152